Chem. Mater. **2000,** *12,* 2930−2935

Hydrothermal Syntheses and X-ray Crystal Structures of Three Inorganic−Organic Hybrid Materials in a Copper Vanadium Phosphate Family: CuL(VO$_2$)(PO$_4$) (L = 4,4′-bipy, 1,10-phen, 2,2′-bipy)

Zhan Shi, Shouhua Feng,* Lirong Zhang, Guoyu Yang, and Jia Hua

Key Laboratory of Inorganic Synthesis and Preparative Chemistry, Jilin University, Changchun 130023, People's Republic of China

Received May 30, 2000

Three inorganic−organic hybrid compounds with the formula CuL(VO$_2$)(PO$_4$), L = 4,4′-bipy, 1,10-phen, and 2,2′-bipy, were hydrothermally synthesized at 160 °C for 120 h and characterized by single-crystal X-ray diffraction. The use of different bidentate organodiamine ligands in initial reaction systems gave rise to the variety in the structures of the products: Cu(4,4′-bipy)(VO$_2$)(PO$_4$) (**1**) and Cu(1,10-phen)(VO$_2$)(PO$_4$) (**2**) crystallize in a monoclinic system with space group $C2/c$, $a = 21.952(4)$ Å, $b = 8.0805(13)$ Å, $c = 15.918(2)$ Å, $\beta = 110.689(4)°$, and $V = 2641.5(7)$ Å^3, and $a = 20.4557(12)$ Å, $b = 11.6231(7)$ Å, $c = 14.6422(8)$ Å, $\beta = 127.5520(10)°$, and $V = 2760.0(3)$ Å^3, respectively. Cu(2,2′- bipy)(VO$_2$)(PO$_4$) (**3**) crystallizes in a triclinic system with space group $P1$, $a = 5.561(5)$ Å, $b = 10.271(9)$ Å, $c = 11.780(9)$ Å, $\alpha = 74.31(3)°$, $\beta = 79.98(3)°$, $\gamma = 85.74(3)°$, and $V = 637.6(9)$ Å^3. The structures of **1** and **2** possess the same {(VO$_2$)(PO$_4$)}$_2$ four-membered rings, whereas the structure of **3** contains {(VO$_2$)(PO$_4$)}$_\infty$ infinite chains. In terms of the organic parts, the {Cu(4,4′-bipy)}$_\infty$ linear chains connect the {(VO$_2$)(PO$_4$)}$_2$ four-membered rings to build up a 3D framework in **1**, whereas the Cu(1,10-phen)$^{2+}$ and Cu(2,2′-bipy)$^{2+}$ fragments link with the {(VO$_2$)(PO$_4$)}$_2$ four-membered rings and {(VO$_2$)(PO$_4$)}$_\infty$ infinite chains to give two 1D structures of **2** and **3**, respectively. Their thermal stabilities were investigated.

Introduction

In the past few years, the design and synthesis of inorganic−organic hybrid materials have been increasingly developed for their potential application in the fields of catalysis, biology, electrical conductivity, magnetism, and photochemistry.[1−9] Current studies on the inorganic−organic hybrid materials mainly concentrate on the following aspects: the template-induced microporous and mesoporous materials, coordination polymers and clusters, and biomineralized systems. This diversity in synthetic systems is derived from the great possibility of the structural construction for both variables of inorganic and organic parts. Apparently, the combination of inorganic and organic components has an infinite array. On the other hand, studies on the reaction mechanisms for the formation of the inorganic−organic hybrid materials have been a great challenge. We have been recently focusing on the extensive synthesis of coordination polymers and clusters in some specific systems, such as the dimensionality change in structure by alternating ligand conformations[10] and the architecture of the [(VO$_2$)(HPO$_4$)]$_\infty$ helical chains in the presence of the 4,4′-bipy ligand.[11] In the cases of coordination complex-linked molybdates, vanadates, and molybdenum phosphates, some one- (1D), two- (2D), and three-dimensional (3D) frameworks,[12,13] such as M$_x$L$_y$/Mo/O,[14−22] M$_x$L$_y$/V/O,[23−29] and M$_x$L$_y$/Mo/P/O[30] (M = transition metal, L = organic ligand) have been syn-

---

* To whom correspondence should be addressed. Fax: +86-431-5671974. E-mail: shfeng@mail.jlu.edu.cn.

(1) Bowes, C. L.; Ozin, G. A. *Adv. Mater.* **1996**, *8*, 13.

(2) Kitagawa, S.; Kondo, M. *Bull. Chem. Soc. Jpn.* **1998**, *71*, 1739.

(3) Chui, S. S.-Y.; Lo, S. M.-F.; Charmant, J. P. H.; Orpen, A. G.; Williams, I. D. *Science* **1999**, *283*, 1148.

(4) Kagan, C. R.; Mitzi, D. B.; Dimitrakopoulos, C. D. *Science* **1999**, *286*, 945.

(5) Batten, S. R.; Robson, R. *Angew. Chem., Int. Ed. Engl.* **1998**, *37*, 1460.

(6) Zaworotko, M. J. *Angew. Chem., Int. Ed. Engl.* **1998**, *37*, 1211.

(7) Janiak, C. *Angew. Chem., Int. Ed. Engl.* **1997**, *36*, 1431.

(8) Hagrman, D.; Hammond, R. P.; Haushalter, R. C.; Zubieta, J. *Chem. Mater.* ***1998***, *10*, 2091.

(9) Fujita, M.; Kwon, Y. J.; Sasake, K.; Yamaguchi, K.; Ogura, K. *J. Am. Chem. Soc.* **1995**, *117*, 7287.

(10) Shi, Z.; Zhang, L.; Gao, S.; Yang, G.; Hua, J.; Gao, L.; Feng, S. *Inorg. Chem.* **2000**, *39*, 1990.

(11) Shi, Z.; Feng, S.; Gao, S.; Zhang, L.; Yang, G.; Hua, J. *Angew. Chem., Int. Ed* **2000**, *39*, 2325.

(12) Hagrman, P. J.; Hagrman, D.; Zubieta, J. *Angew. Chem., Int. Ed.* **1999**, *38*, 2638.

(13) Chesnut, D. J.; Hagrman, D.; Zapf, P. J.; Hammond, R. P.; LaDuca, R. L., Jr.; Haushalter, R. C.; Zubieta, J. *Coord. Chem. Rev.* **1999**, *192*, 737.

(14) Hagrman, D.; Zubieta, C.; Rose, D. J.; Zubieta, J.; Haushalter, R. C. *Angew. Chem., Int. Ed. Engl.* **1997**, *36*, 873.

(15) Zapf, P. J.; Warren, C. J.; Haushalter, R. C.; Zubieta, J. *Chem. Commun.* **1997**, 1543.

(16) Hagrman, D.; Sangregorio, C.; O'Connor, C. J.; Zubieta, J. *J. Chem. Soc., Dalton Trans.* **1998**, 3707.

(17) Hagrman, D.; Zapf, P. J.; Zubieta, J. *Chem. Commun.* **1998**, 1283.

(18) Hagrman, D.; Zubieta, J. *Chem. Commun.* **1998**, 2005.

(19) Zapf, P. J.; Hammond, R. P.; Haushalter, R. C.; Zubieta, J. *Chem. Mater.* **1998**, *10*, 1366.

(20) Hagrman, D.; Warren, C. J.; Haushalter, R. C.; Seip, C.; O'Connor, C. J.; Rarig, R. S., Jr.; Johnson, K. M., III; LaDuca, R. L., Jr.; Zubieta, J. *Chem. Mater.* **1998**, *10*, 3294.

10.1021/cm000429p CCC: $19.00

Table 1. Summary of Crystal Data for Cu(4,4′-bipy)(VO$_2$)(PO$_4$) (1), Cu(1,10-phen)(VO$_2$)(PO$_4$) (2), and Cu(2,2′-bipy)(VO$_2$)(PO$_4$) (3)

	1	**2**	**3**
emp formula	$C_{10}H_8N_2CuVPO_6$	$C_{12}H_8N_2CuVPO_6$	$C_{10}H_8N_2CuPVO_6$
formula wt	397.63	421.65	397.63
crystal system	monoclinic	monoclinic	triclinic
space group	*C*2/*c*	*C*2/*c*	$P\bar{1}$
a (Å)	21.952(4)	20.4557(12)	5.561(5)
b (Å)	8.0805(13)	11.6231(7)	10.271(9)
c (Å)	15.918(2)	14.6422(8)	11.780(9)
α (deg)	90	90	74.31(3)
β (deg)	110.689(4)	127.5520(10)	79.98(3)
γ (deg)	90	90	85.74(3)
V (Å^3)	2641.5(7)	2760.0(3)	637.6(9)
Z	8	8	2
D_{calc} (g cm^{-3})	2.000	2.030	2.071
μ (mm^{-1})	2.467	2.367	2.555
data/restraints parameters	1923/0/222	1984/0/240	1508/0/222
final *R* indices [$I > 2\sigma(I)$]: R_1,^{a} $_wR_2$^{b}	0.0444, 0.1228	0.0330, 0.0754	0.0426, 0.1132

^{a} $R_1 = \sum||F_o| - |F_c||/\sum|F_o|$. ^{b} $_wR_2 = [\sum[w(F_o^2 - F_c^2)^2]/\sum[w(F_o^2)^2]]^{1/2}$.

thesized, but there were less studies to understand the influence of inorganic and organic parts on the formation of a framework. In this study, we selected V−P−O as an inorganic part and varied the organic parts (ligands or transition metal coordination complexes). The transition metal coordination complexes may function as templates to direct or bridge the structure of the polyoxoanion blocks, chains, and layers, and thus the use of suitable coordination complexes is expected to be a key factor for the formation of an inorganic−organic framework. We report here the hydrothermal syntheses and X-ray crystal structures of three novel inorganic−organic hybrid materials in a family: CuL(VO$_2$)(PO$_4$), L = 4,4′-bipy (**1**), 1,10-phen (**2**), and 2,2′-bipy (**3**).

Experimental Section

Synthesis and Characterization. All syntheses were carried out in 20 mL Teflon-lined stainless steel vessels under autogenous pressure with a filling capacity of ~50%. The elemental analysis was performed on a Perkin-Elmer 2400 element analyzer, and inductively coupled plasma (ICP) analysis was performed on a Perkin-Elmer Optima 3300DV ICP spectrometer. Infrared spectra were obtained on a Nicolet 5DX FT-IR instrument. A Perkin-Elmer DTA 1700 differential thermal analyzer and a Perkin-Elmer TGA 7 thermogravimetric analyzer were used to obtain DTA and TGA curves in air with a temperature increasing rate of 10 °C min^{-1}.

Synthesis of Cu(4,4′-bipy)(VO$_2$)(PO$_4$) (1). A mixture of NaVO$_3$·2H$_2$O (0.158 g), NaH$_2$PO$_4$·2H$_2$O (0.156 g), Cu(NO$_3$)$_2$·6H$_2$O (0.291 g), 4,4′-bipy·2H$_2$O (0.192 g), and H$_2$O (10 mL) in a molar ratio of 1:1:1:1:556 was heated at 160 °C for 120 h to give light blue crystals of **1**. Anal. Calcd for $C_{10}H_8N_2CuVPO_6$: C, 30.20; H, 2.03; N, 7.04; Cu, 15.98; V, 12.81; P, 7.79. Found: C, 29.99; H, 2.18; N, 6.86; Cu, 15.89; V, 12.97; P, 7.86. IR (KBr pellet, cm^{-1}): 1611 (s), 1537 (m), 1416 (m), 1217 (m), 1157 (s), 1063 (s), 1009 (s), 956 (s), 918 (s), 875 (m), 819 (s), 732 (m), 714 (m), 650 (m), 603 (m), 576 (m), 508 (s), 440 (m).

Synthesis of Cu(1,10-phen)(VO$_2$)(PO$_4$) (2). A mixture of NaVO$_3$·2H$_2$O (0.158 g), NaH$_2$PO$_4$·2H$_2$O (0.156 g), Cu(NO$_3$)$_2$·6H$_2$O (0.291 g), 1,10-phen·H$_2$O (0.198 g), and H$_2$O (10 mL) in a molar ratio of 1:1:1:1:556 was heated at 160 °C for 120 h to give light blue crystals of **3**. Anal. Calcd for $C_{12}H_8N_2CuVPO_6$: C, 34.18; H, 1.91; N, 6.64; Cu, 15.07; V, 12.08; P, 7.35. Found: C, 34.01; H, 1.82; N, 6.53; Cu, 15.15; V, 12.21; P, 7.42. IR (KBr pellet, cm^{-1}): 1625 (m), 1578 (w), 1518 (w), 1428 (m), 1215 (m), 1164 (s), 1108 (m), 1074 (m), 1054 (m), 1017 (s), 965 (s), 928 (m), 916 (m), 873 (m), 852 (m), 782 (m), 740 (m), 722 (m), 662 (m), 620 (m), 521 (m), 434 (m).

Synthesis of Cu(2,2′-bipy)(VO$_2$)(PO$_4$) (3). A mixture of NaVO$_3$·2H$_2$O (0.158 g), NaH$_2$PO$_4$·2H$_2$O (0.156 g), Cu(NO$_3$)$_2$·6H$_2$O (0.291 g), 2,2′-bipy (0.156 g), and H$_2$O (10 mL) in a molar ratio of 1:1:1:1:556 was heated at 160 °C for 120 h to give light blue crystals of **3**. Anal. Calcd for $C_{10}H_8N_2CuVPO_6$: C, 30.20; H, 2.03; N, 7.04; Cu, 15.98; V, 12.81; P, 7.79. Found: C, 30.01; H, 2.16; N, 6.88; Cu, 16.09; V, 12.72; P, 7.89. IR (KBr pellet, cm^{-1}): 1646 (m), 1606 (m), 1570 (m), 1497 (m), 1473 (m), 1445 (m), 1317 (m), 1250 (m), 1177 (s), 1074 (s), 1032 (m), 1003 (s), 958 (s), 933 (s), 891 (s), 799 (m), 772 (m), 729 (m), 637 (m), 621 (m), 567 (m), 511 (s), 465 (m), 426 (m), 409 (m).

The infrared spectra of compounds **1**, **2**, and **3** exhibit characteristic ligand bands in the 1100−1600 cm^{-1} region; the compounds also possess a strong intensive band at 1009 cm^{-1} (**1**), 1017 cm^{-1} (**2**), and 1003 cm^{-1} (**3**) attributed to ν(P−O) and a band at 956 cm^{-1} (**1**), 965 cm^{-1} (**2**), and 958 cm^{-1} (**3**) attributed to ν(V−O).

Determination of Crystal Structures. Crystals of **1**−**3** suitable for single-crystal X-ray diffraction with size 0.400 mm × 0.200 mm × 0.200 mm, 0.280 mm × 0.280 mm × 0.120 mm, and 0.250 mm × 0.090 mm × 0.090 mm were selected, respectively. Structural analyses for **1**−**3** were performed on a Siemens SMART CCD diffractometer using graphite monochromated Mo Kα radiation (λ (Mo Kα) = 0.71073 Å). The data were collected at 20 ± 2 °C. Date processing was accomplished with the SAINT processing program.[31] Direct methods were used to solve structures using the SHELXTL crystallographic software package.[32] Hydrogen atoms were located by difference Fourier map. All non-hydrogen atoms were refined anisotropically.

Experimental X-ray data for structures **1**−**3** are listed in Table 1; atomic coordinates with isotropic temperature factors,

---

(21) Hagrman, D.; Hagrman, P. J.; Zubieta, J. *Angew. Chem., Int. Ed. Engl.* **1999**, *38*, 3165.

(22) Hagrman, P. J.; Zubieta, J. *Inorg. Chem.* **1999**, *38*, 4480.

(23) Zhang, Y.; DeBord, J. R. D.; O'Connor, C. J.; Haushalter, R. C.; Clearfield, A.; Zubieta, J. *Angew. Chem., Int. Ed. Engl.* **1996**, *35*, 989.

(24) DeBord, J. R. D.; Haushalter, R. C.; Meyer, L. M.; Rose, D. J.; Zapf, P. J.; Zubieta, J. *Inorg. Chim. Acta* **1997**, *256*, 165.

(25) Hagrman, P. J.; Bridges, C.; Greedan, J. E.; Zubieta, J. *J. Chem. Soc., Dalton Trans.* **1999**, 2901.

(26) LaDuca, R. L., Jr.; Finn, R.; Zubieta, J. *Chem. Commun.* **1999**, 1669.

(27) Zheng, L. M.; Zhao, J. S.; Lii, K. H.; Zhang, L. Y.; Liu, Y.; Xin, X. Q. *J. Chem. Soc., Dalton Trans.* **1999**, 939.

(28) Shi, Z.; Zhang, L.; Zhu, G.; Hua, J.; Ding, H.; Feng, S. *Chem. Mater.* **1999**, *11*, 3565.

(29) Zhang, L.; Shi, Z.; Yang, G.; Chen, X.; Feng, S. *J. Chem. Soc., Dalton Trans.* **2000**, 275.

(30) Lu, J.; Xu, Y.; Goh, N. K.; Chia, L. S. *Chem. Commun.* **1998**, 2733.

(31) SHELXTL, Version 5.1; Siemens Industrial Automation, Inc.: 1997.

(32) Software packages SMART and SAINT; Siemens Analytical X-ray Instruments Inc.: Madison, WI, 1996.

full tables of bond lengths and angles, and anisotropic temperature factors are available in the Supporting Information.

Results and Discussion

Synthesis. By exploiting hydrothermal synthesis,[33−38] a variety of inorganic−organic hybrid materials, including 1D, 2D, and 3D structures, have been reported.[13−30] To investigate the influence of ligands on the formation of an inorganic−organic hybrid compound, we selected three bidentate organodiamine ligands (4,4′-bipy, 1,10-phen, or 2,2′-bipy) and kept other reactants and experimental conditions the same. In such a specific hydrothermal process, many factors may affect the formation and crystal growth of products, such as the type of initial reactants, pH value, reaction time, and temperature. In our case, the use of dihydrogenphosphate ($NaH_2PO_4 \cdot 2H_2O$) as a phosphoric source was of crucial importance for the crystallization of products. This is explained by the need for a certain pH value for the formation of vanadium species and coordinated complexes. NaH_2PO_4 acts not only as a phosphoric source but also as an adjuster for the pH of the reaction system. The pH value of the reaction system is ~4.0 at the beginning of the reaction and ~5.0 at the end of the reaction. The experimental conditions differ only by changing three different bidentate organodiamine ligands (4,4′-bipy, 1,10-phen, and 2,2′-bipy), which lead to three different novel structures. In our hydrothermal system, although the crystallization mechanism may be complicated, the formation reaction of **1**−**3** could be proposed as follows:

$$\begin{aligned} &NaVO_3 + NaH_2PO_4 + Cu(NO_3)_2 + L = \\ &\qquad CuL(VO_2)(PO_4) + 2NaNO_3 + H_2O \\ &\qquad\qquad L = 4,4'\text{-bipy, 1,10-phen, and } 2,2'\text{-bipy} \end{aligned}$$

From the observation of the increase of the pH value from 4 to 5 in reaction systems, we may consider the reaction as a hydrox-oxo-polymerization process.

Structural Description. The structure of **1** has a 3D framework, consisting of infinite layers of Cu/V/P/O, linked by the coordination of 4,4′-bipy with Cu atoms. The fundamental structural motif is shown in Figure 1a. Four-membered rings (4-MRs), $\{(VO_2)(PO_4)\}_2$, are basic subunits on the layers, composed of alternative corner-sharing VO_4 and PO_4 tetrahedra. The Cu coordination geometry is a square-pyramidal configuration, which is defined by two trans nitrogen donors of 4,4′-bipy, two oxygen donors of phosphate in the basal plane, and an oxygen of vanadate in the apical position. Through a Cu−O=V (Cu−O, 2.436 Å; V=O, 1.633 Å) and two Cu−O=P (Cu−O, 1.929, 1.962 Å; P=O, 1.509, 1.525 Å) bridges, the $\{(VO_2)(PO_4)\}_2$ units were linked to produce an inorganic layer motif $\{CuV_2P_2O_{12}\}_\infty$ in the (100) plane, as shown in Figure 1b. The axial Cu−O bond (Cu−O, 2.436 Å) is considerably longer than the equatorial ones (Cu−O, 1.929, 1.962 Å) due to Jahn−Teller distortion. The remaining oxygen of the VO_4 tetrahedra is a terminal oxygen with a V=O distance of 1.614 Å. The 4,4′-bipy ligands bridge the Cu site to form a 1D $\{Cu(4,4'\text{-bipy})\}_n^{2n+}$ chain. Combining the 1D $\{Cu(4,4'\text{-bipy})\}_n^{2n+}$ and 4-MRs $\{(VO_2)(PO_4)\}_2$ results in the overall 3D framework structure (Figure 1c). Alternatively, the structure may be viewed as the bridging

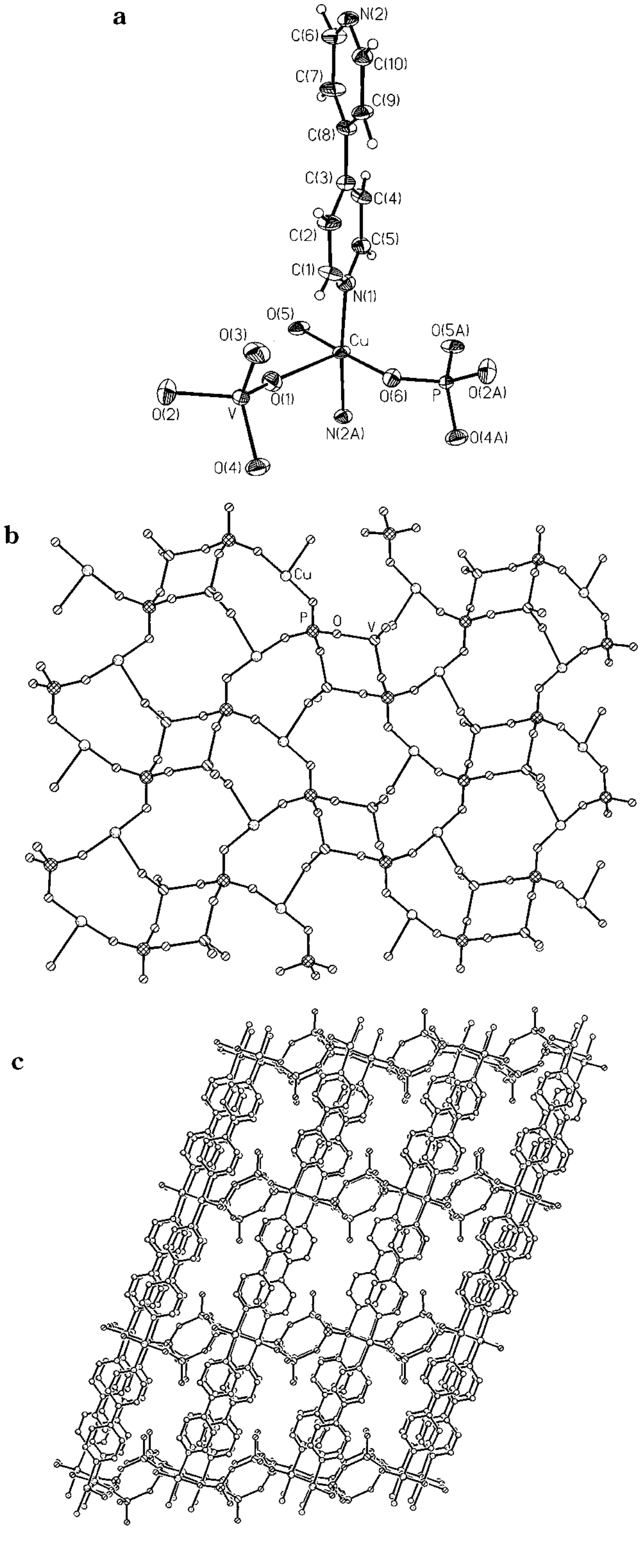

Figure 1. **(**a**)** View of the coordination environments of the copper, vanadium, and phosphorus atoms in **1**, showing the atom-labeling scheme and 50% thermal ellipsoids. **(**b**)** View parallel to the *a* axis of the $\{CuV_2P_2O_{12}\}$ layer of **1**. **(**c**)** View along the *b* axis, showing the virtual channels.

---

(33) Feng, S.; Greenblatt, M. *Chem. Mater.* **1993**, *5*, 1277.

(34) Li, G.; Feng, S.; Li, L.; Li, X.; Jin, W. *Chem. Mater.* **1997**, *9*, 2894.

(35) Xun, X.; Feng, S.; Wang, J.; Xu, R. *Chem. Mater.* **1997**, *9*, 2966.

(36) Pang, G.; Feng, S.; Tang, Y.; Tan, C.; Xu, R. *Chem. Mater.* **1998**, *10*, 2446.

(37) Zhao, H.; Feng, S. *Chem. Mater.* **1999**, *11*, 958.

(38) Zhang, L.; Shi, Z.; Yang, G.; Chen, X.; Feng, S. *J. Solid State Chem.* **1999**, *148*, 450.

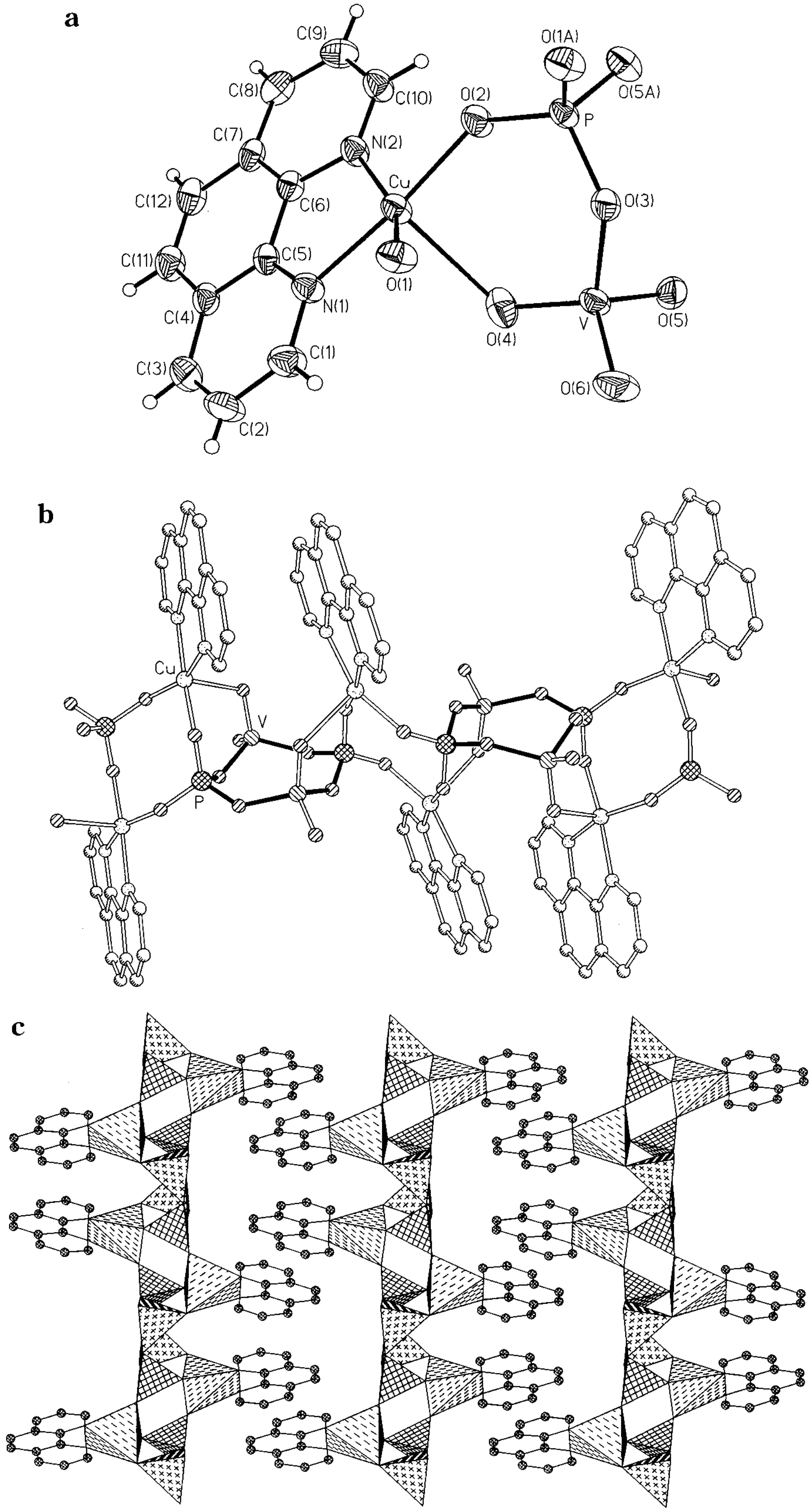

Figure 2. (a) View of the coordination environments of the copper, vanadium, and phosphorus atoms in **2**, showing the atom-labeling scheme and 50% thermal ellipsoids. (b) View of the one-dimensional chains of **2** along the *c* axis. (c) View of the packing of adjacent one-dimensional chains, showing the stacking of phen from adjacent chains in **2**.

of 4,4′-bipy ligands, which are coordinated with Cu atoms, with adjacent Cu/V/P/O layers to generate a 3D framework. The pyridine rings of 4,4′-bipy linking two coppers are twisted by 38.5°. The bridged Cu−Cu distance along 4,4′-bipy is 11.055 Å. The distance between adjacent 4,4′-bipy ligands is between 4.2 and 9.4 Å. Accordingly, channels along the (010) directions are formed.

As expected, the replacement of 4,4′-bipy by 1,10-phen made the structure change from 3D to 1D. The structure of **2** is constructed from two subunits, for example, $\{(VO_2)(PO_4)\}_2^{2-}$ 4-MRs which are the same as those shown in **1** and Cu(1,10-phen)$^{2+}$ fragments. As shown in Figure 2a, the Cu center exhibits a $\{CuN_2O_3\}$ square-pyramidal coordination geometry by bonding to two cis nitrogen donors (Cu−N, 2.008 and 2.018 Å) of 1,10-phen, two oxygen donors (Cu−O, 1.908 and 1.925 Å) of phosphate in the basal plane, and an oxygen (Cu−O, 2.435 Å) of vanadate in the apical position. Oxygen atoms, from two adjacent VO_4 and PO_4 tetrahedra of $\{V_2P_2O_4\}$ 4-MRs, bond to the copper atom to form $\{CuVPO_3)$ 3-MRs, and the remaining oxygen bridges PO_4 tetrahedra from other $\{V_2P_2O_4\}$ 4-MRs, forming $\{Cu_2P_2O_4\}$ 4-MRs. As a result, a zigzag chain along the *c* axis is generated in a sequence of $\{CuVPO_3)$ 3-MRs, $\{V_2P_2O_4\}$ 4-MRs, $\{CuVPO_3\}$ 3-MRs, and $\{Cu_2P_2O_4\}$ 4-MRs (Figure 2b). The adjacent chains of $\{Cu(l,10\text{-}phen)(VO_2)(PO_4)\}_\infty$ are in a close connection through so-called $\pi-\pi$ interactions of the 1,10-phen as shown in Figure 2c. The close contact distance between adjacent rings in **2** is 3.4 Å.

The structure of **3** consists of two $\{(VO_2)(PO_4)\}_\infty$ chains linked by Cu(2,2′-bipy)$^{2+}$ fragments into a pair of 1D chains. Figure 3a shows a thermal ellipsoid plot of the coordination states of Cu, V, and P atoms. Vanadium and phosphorus sites are still tetrahedral, but their alternate connection forms $\{(VO_2)(PO_4)\}_\infty$ infinite chains by corner-sharing oxygen atoms, instead of $\{(VO_2)(PO_4)\}_2$ 4-MRs. As in **2**, the Cu square-pyramidal coordination geometry is defined by two cis nitrogen donors (Cu−N, 1.996 and 1.999 Å) of 2,2′-bipy, two oxygen donors (Cu−O, 1.918 and 1.922 Å) of phosphate in the basal plane, and an oxygen (Cu−O, 2.351 Å) of vanadate in the apical position. Three oxygen atoms from adjacent VO_4 and PO_4 on a chain, and a PO_4 on another chain bond to a copper atom and form a pair of 1D chains (see Figure 3b). In the 1D chains, the pyridyl groups from adjacent 2,2′-bipy ligands interdigitate and provide weak $\pi-\pi$ stacking interactions (ca. 3.5 Å average interplanar separations). Figure 3c shows the packing arrangement of the 1D chains.

Bond-length and bond-strength calculations were based on the method and data of Brown, Shannon, and Altermatt.[39,40] The bond valence sums for V are 5.03 (in **1**), 5.09 (in **2**), and 5.02 (in **3**), respectively, indicating all V atoms are pentavalent.

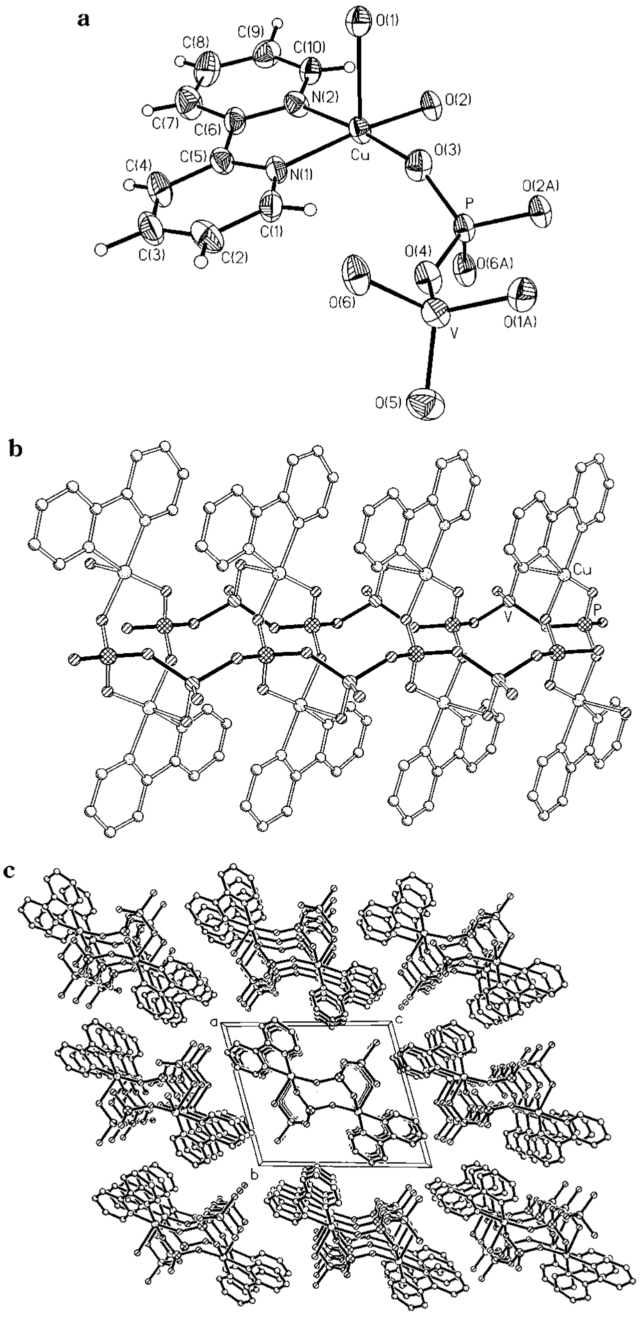

Figure 3. (a) View of the coordination environments of the copper, vanadium, and phosphorus atoms in **3**, showing the atom-labeling scheme and 50% thermal ellipsoids. **(b)** View of the pairs of one-dimensional chains in **3**. (c) View of the packing of **3** with the unit cell outlined.

Organic ligands dominate the dimensionality of an inorganic−organic hybrid compound by affecting both the arrangement of inorganic units and the coordinate characteristics of forming complexes. It is noteworthy that the structures of compounds **1**, **2**, and **3** differ from those of the recently reported $Co(4,4'\text{-}bipy)_2(VO_2)_2(HPO_4)_4$ (**4**) and $Ni(4,4'\text{-}bipy)_2(VO_2)_2(HPO_4)_4$ (**5**), even though their compositions are similar. Table 2 summarizes the structural characteristics and compositions of related M_xL_y/V/P/O compounds. Compounds **1**−**3** all share a motif which consists of $\{PO_4\}$ tetrahedral, $\{VO_4\}$ tetrahedral, and $\{CuN_2O_3\}$ square-pyramidal units. In compound **1**, 4,4′-bipy as a rigid unit reacts with copper ions to form a polymeric coordination cation $\{Cu(4,4'\text{-}bipy)\}_\infty$. These $\{Cu(4,4'\text{-}bipy)\}_\infty$ cations are bridged by $\{(VO_2)(PO_4)\}_2$ 4-MRs in inorganic layers $\{CuV_2P_2O_{12}\}_\infty$ to form a 3D framework (**1**). Therefore, the $\{Cu(4,4'\text{-}bipy)\}_\infty$ is most important for the formation of the 3D structure of **1**. In compounds **2** and **3**, the chelating bipy ligand (1,10-phen or 2,2′-bipy), which occupies the coordination sphere on copper, prevents the formation of the 3D structure. The {Cu(1,10-phen)} and {Cu(2,2′-bipy)} fragments link the $\{(VO_2)(PO_4)\}_2$ 4-MRs or $\{(VO_2)(PO_4)\}_\infty$ chains through central copper to form 1D structures (**2** or **3**). Compounds **4** and **5**, which were synthesized in our group, have a 3D structure constructed from $[(VO_2)(HPO_4)]_\infty$ helical chains and $[M(4,4'\text{-}bipy)_2]^{2+}$ (where M = Co, Ni) fragments. The M atom exists in octahedral $\{MN_2O_4\}$ coordinated with two trans nitrogen donors from two different 4,4′-bipy

---

(39) Brown, I. D.; Shannon, R. D. *Acta Crystallogr.* **1973**, *A29*, 266.
(40) Brown, I. D.; Altermatt, D. *Acta Crystallogr.* **1985**, *B41*, 244.

Table 2. Comparison of Structures for the M_xL_y/V/P/O System (M = transition metal, L = organic ligand)

compound	structural type	metal/ligand description	metal coordination geometry	V/P/O description	ref
Cu(4,4′-bipy)(VO_2)(PO_4)	3D	{Cu(4,4′-bipy)}$_n^{2n+}$ 1D chain	{CuN_2O_3} square-pyramidal	[(VO_2)(PO_4)]$_2$ four-membered ring	this work
Cu(1,10-phen)(VO_2)(PO_4)	1D	{Cu(1,10-phen)}$^{2+}$ fragment	{CuN_2O_3} square-pyramidal	[(VO_2)(PO_4)]$_2$ four-membered ring	this work
Cu(2,2′-bipy)(VO_2)(PO_4)	1D	{Cu(2,2′-bipy)}$^{2+}$ fragment	{CuN_2O_3} square-pyramidal	[(VO_2)(PO_4)]$_\infty$ 1D chain	this work
Co(4,4′-bipy)$_2$(VO_2)$_2$(HPO_4)$_4$	3D	{Co(4,4′-bipy)$_2$}$^{2+}$ fragment	{CoN_2O_4} octahedral	[(VO_2)(HPO_4)]$_\infty$ helical chain	11
Ni(4,4′-bipy)$_2$(VO_2)$_2$(HPO_4)$_4$	3D	{Ni(4,4′-bipy)$_2$}$^{2+}$ fragment	{NiN_2O_4} octahedral	[(VO_2)(HPO_4)]$_\infty$ helical chain	11

molecules. The remaining nitrogen donors of the 4,4′-bipy molecules link the [(VO_2)(HPO_4)]$_\infty$ chains through the N−V bonds. The interaction of the [M(4,4′-bipy)$_2$] fragment with each vanadium atom on the [(VO_2)(HPO_4)]$_\infty$ chains is very important for the formation of a helix. The isolation and characterization of compounds **1**−**5** confirmed the observation that an organic ligand may profoundly influence the structures of polyoxoanion subunits. Furthermore, the selection of a metal center, certain coordination preferences, ligand donor group geometry, and the structure of polyoxoanion subunits constitute other factors to affect the formation of unique structures of inorganic−organic hybrid compounds.

Thermal Analysis. Compounds **1** and **2** are thermally stable up to ∼200 °C, and compound **3** is stable up to ∼300 °C. The TGA−DTA of compound **1** showed that the 4,4′-bipy molecule was combusted from the crystal in the range 230−550 °C with weight losses of 41.0% in three steps (calculated value of 39.27%). The TGA−DTA of compound **2** indicated that the 1,10-phen ligand was lost in three steps on heating with weight losses of 41.5% at 240−520 °C (calculated value of 42.73%). The TGA−DTA of **3** exhibited a weight loss of 40.2% in the range 310−520 °C, corresponding to the loss of the 2,2′-bipy ligands (calculated value of 39.27%).

Conclusions

The successful hydrothermal isolation of inorganic−organic compounds **1**−**3** has provided novel examples of linked vanadium phosphate through the metal coordination complex. Three different bidentate organodiamine ligands (4,4′-bipy, 1,10-phen, and 2,2′-bipy) led to three novel structures. It is evident that a hydrothermal technique offers a powerful method for the synthesis of the modified metal oxide structures and for the isolation of new inorganic−organic hybrid materials. We are currently carrying out the substitution of copper for other metals in similar hydrothermal systems and trying to find a clue to the rational synthesis of some new inorganic−organic materials.

Acknowledgment. This work was supported by the National Natural Science Foundation of China and the STMC through a key project of Rational Synthesis of Inorganic−Organic Materials.

Supporting Information Available: Tables of experimental conditions, atomic positional parameters, bond lengths and angles, anisotropic temperature factors, and calculated hydrogen atom positions and TGA−DTA traces for **1**−**3** (PDF). This material is available free of charge via the Internet at http://pubs.acs.org.

CM000429P